PNAS RESEARCH ARTICLE | IMMUNOLOGY AND INFLAMMATION OPEN ACCESS

Human anti-C1q autoantibodies bind specifically to solid-phase C1q and enhance phagocytosis but not complement activation

Douwe J. Dijkstra[a,1], Fleur S. van de Bovenkamp[a,b], Leoni Abendstein[c], Rob Zuijderduijn[a], Jos Pool[a], Cynthia S. M. Kramer[a], Linda M. Slot[d], Jan W. Drijfhout[a], Lisanne de Vor[e], Kyra A. Gelderman[f], Suzan H. M. Rooijakkers[e], Arnaud Zaldumbide[c], Gestur Vidarsson[g], Thomas H. Sharp[c], Paul W. H. I. Parren[a,h], and Leendert A. Trouw[a,1]

Edited by Douglas Fearon, Cold Spring Harbor Laboratory, Cold Spring Harbor, NY; received June 26, 2023; accepted October 27, 2023

Autoantibodies directed against complement component C1q are commonly associated with autoimmune diseases, especially systemic lupus erythematosus. Importantly, these anti-C1q autoantibodies are specific for ligand-bound, solid-phase C1q and do not bind to fluid-phase C1q. In patients with anti-C1q, C1q levels are in the normal range, and the autoantibodies are thus not depleting. To study these human anti-C1q autoantibodies at the molecular level, we isolated C1q-reactive B cells and recombinantly produced nine monoclonal antibodies (mAbs) from four different healthy individuals. The isolated mAbs were of the IgG isotype, contained extensively mutated variable domains, and showed high affinity to the collagen-like region of C1q. The anti-C1q mAbs exclusively bound solid-phase C1q in complex with its natural ligands, including immobilized or antigen-bound IgG, IgM or CRP, and necrotic cells. Competition experiments reveal that at least 2 epitopes, also targeted by anti-C1q antibodies in sera from SLE patients, are recognized. Electron microscopy with hexameric IgG-C1q immune complexes demonstrated that multiple mAbs can interact with a single C1q molecule and identified the region of C1q targeted by these mAbs. The opsonization of immune complexes with anti-C1q greatly enhanced Fc-receptor-mediated phagocytosis but did not increase complement activation. We conclude that human anti-C1q autoantibodies specifically bind neo-epitopes on solid-phase C1q, which results in an increase in Fc-receptor-mediated effector functions that may potentially contribute to autoimmune disease immunopathology.

complement | autoantibody | anti-C1q | autoimmunity

Significance

Autoantibodies against complement component C1q are associated with several autoimmune diseases.These autoantibodies specifically bind to ligand-bound, solid-phase C1q, but not fluid-phase C1q. We identified nine human anti-C1q clones from healthy individuals and produced them recombinantly. We found that these autoantibodies recognize the collagen-like region of solid-phase C1q, when C1q is in complex with a range of its natural ligands. Electron microscopy revealed that multiple antibodies bind a single C1q molecule and further identified the region of C1q targeted by these mAbs. Binding of anti-C1q does not increase complement activation on immune complexes; however, we demonstrated that anti-C1q autoantibodies bound to solid-phase C1q can activate immune cells by engaging Fc-receptors. Anti-C1q autoantibodies may thereby contribute to pathological processes in autoimmune disease.

The complement system plays an important role in both innate immune defense and the development of adaptive immune responses. In addition, complement is involved in the clearance of immune complexes, cellular debris, and tissue remodeling (1). In the classical pathway of complement activation, the recognition molecule C1q binds a wide array of ligands, including target-bound immunoglobulins (Ig) and C-reactive protein (CRP), which trigger the activation of the C1 enzymes C1r and C1s and propagation of the complement cascade. The function of C1q in normal physiology is underscored by the clinical presentation of C1q-deficient patients with infections and systemic lupus erythematosus (SLE)-like disease (2). Excessive complement activation is thought to be a major pathological mechanism of several rheumatic autoimmune diseases including SLE (3).

Autoantibodies targeting specific complement proteins have been detected in several autoimmune disorders (4). Anti-C1q autoantibodies have been found to be prevalent in hypocomplementemic urticarial vasculitis syndrome (HUVS; 100% of the patients) and in SLE (around 40% of the patients)(reviewed in refs. (5, 6)). In SLE, the presence of anti-C1q autoantibodies is associated with lupus nephritis (7–9). Interestingly, anti-C1q autoantibodies are also present in a substantial fraction of the healthy population, indicating that anti-C1q autoantibodies may only be pathogenic in certain circumstances (10, 11). Indeed, experiments in mice indicate that anti-C1q autoantibodies only induce damage to the kidney when C1q is already present on deposited immune complexes (7). Anti-C1q autoantibodies are measured in routine diagnostics, but require tailored experimental conditions to avoid binding of immune complexes to the immobilized C1q (12). The detection of anti-C1q autoantibodies is therefore performed in buffers containing a high concentration of NaCl, as this prevents ligand binding of C1q, while largely retaining the binding of anti-C1q autoantibodies (13).

The molecular characteristics of anti-C1q autoantibodies are currently unknown, but studies on patient sera indicated a specificity for solid-phase C1q (14). The term solid-phase C1q is used in the literature to describe C1q bound to any ligand or surface (14). During complement initiation, C1q undergoes a conformational change upon binding to its ligands, which reveals neo-epitopes to which antibodies specific for solid-phase C1q can

Competing interest statement: D.J.D. and L.A.T. are coinventors on a patent application describing antibodies against complement protein C1q.

This article is a PNAS Direct Submission.

[1]To whom correspondence may be addressed. Email: d.j.dijkstra@lumc.nl or l.a.trouw@lumc.nl.

This article contains supporting information online at https://www.pnas.org/lookup/suppl/doi:10.1073/pnas.2310666120/-/DCSupplemental.

Published December 4, 2023.

bind (15) (Fig. 1*A*). Several studies using serum from SLE patients have reported that anti-C1q autoantibodies mainly target the collagen-like region (CLR) as opposed to the globular head (GH) domains (16, 17). A few reports described that autoantibodies against GH polypeptides can also be present in some individuals (18, 19), and another report described epitope mapping using linear peptides (20).

Most studies characterizing anti-C1q autoantibodies have focused on polyclonal antibodies from serum of human donors, either patients or healthy individuals. An investigation into monoclonal human anti-C1q to analyze anti-C1q autoantibody responses on a molecular and functional level is therefore warranted. We set out to isolate single anti-C1q-positive B cells, clone them, and recombinantly produce human monoclonal antibodies (mAbs). In total, we generated nine anti-C1q human mAbs, recognizing two distinct epitopes on the CLR of solid-phase C1q. We demonstrate that the epitopes targeted by the anti-C1q mAbs constitute the same epitopes targeted by anti-C1q autoantibodies present in SLE sera. Our study may lead to diagnostics or therapeutics for the treatment of complement-mediated inflammatory and autoimmune diseases and may provide insight into the immunopathological processes that drive lupus nephritis.

Results

Isolation of Anti-C1q-positive B Cells from Peripheral Blood. To select possible donors for C1q-reactive B cells, sera from healthy donors and SLE patients were screened for the presence of anti-C1q autoantibodies. We identified five healthy donors and 11 SLE patients with anti-C1q autoantibodies, who were used for isolating B cells (Fig. 1*C*). Single B cells from these anti-C1q positive donors were FACS sorted for C1q reactivity using soluble immunocomplexes presenting C1q in solid-phase. Therefore, the cells were stained using C1q bound to pre-formed IgG hexamers against DNP which were detected with DNP-biotin in complex with either PE or AlexaFluor647. We sorted the cells double positive for PE and AlexaFluor647. Sorted cells were cultured and supernatant was screened for anti-C1q IgG, resulting in the successful identification of nine unique anti-C1q mAbs from healthy donors.

Variable domains of anti-C1q mAbs were sequenced and analyzed in IMGT V-quest to determine mutational load and V(D)J gene usage. The number of mutations in the V genes (up to 37) suggests that several of the isolated anti-C1q mAbs had undergone substantial somatic hypermutation (Table 1). The antibody variable domain analysis showed diversity in putative V(D)J gene usage, even between clones isolated from the same donor. Only mAbs 4D2 and 4E6 from donor 2 were highly similar and likely derived from a common ancestor B cell.

Anti-C1q mAbs were expressed recombinantly in the eukaryotic Expi293 expression system and purified for further analysis. Binding of the mAbs in C1q-coated enzyme-linked immunosorbent assay (ELISA) varied greatly, with more than 100-fold difference in mAb binding to C1q comparing the strongest and the weakest binder (Fig. 1*D*). To exclude the possibility that the selected mAbs were polyreactive, binding to several well-known

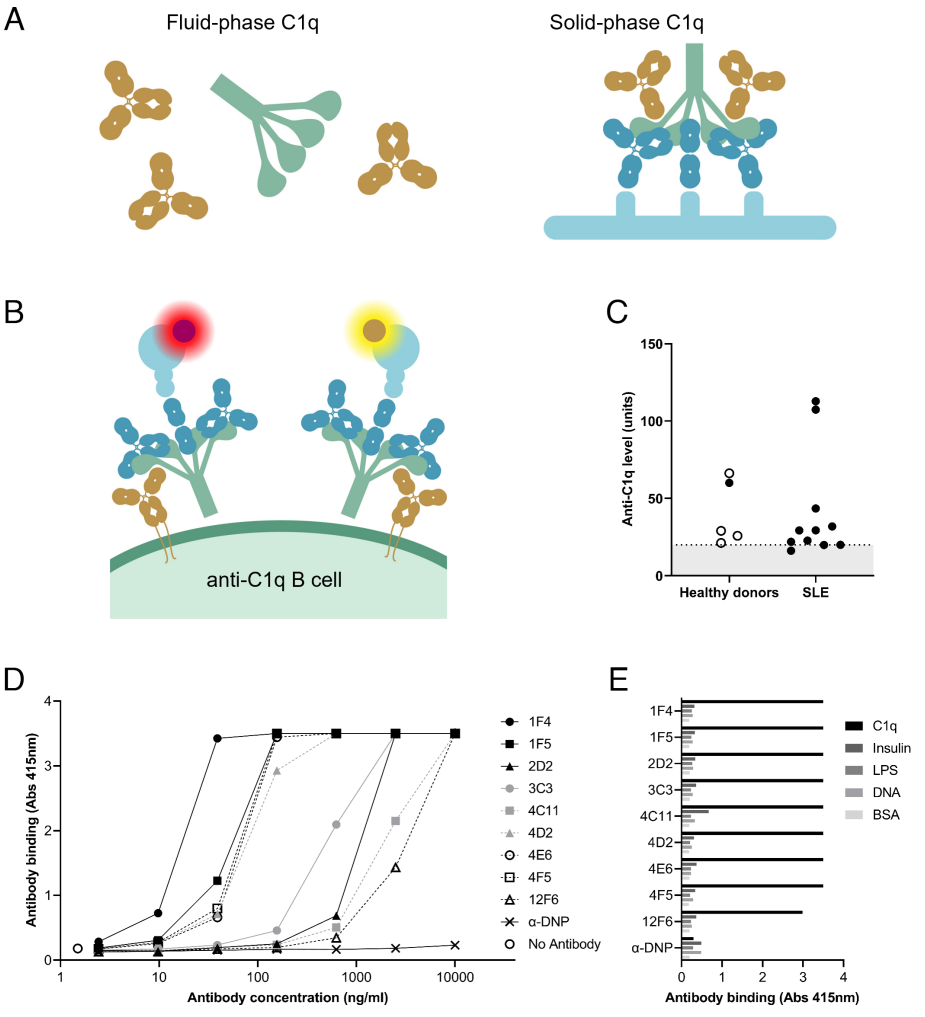

Fig. 1. Human solid-phase C1q autoantibodies were cloned from several healthy donors. (*A*) Anti-C1q antibodies do not bind to fluid-phase C1q (*Left*) but do bind to solid-phase C1q (*Right*), which is the conformation C1q adopts upon binding to a ligand or surface. (*B*) Schematic overview of the staining complex used for sorting anti-C1q-specific B cells. C1q (green) is in a solid-phase conformation in complex with hexameric anti-DNP IgG (dark blue), which binds fluorescently labeled streptavidin via a DNP- and biotin-containing peptide (light blue). Streptavidin was labeled with either PE (yellow) or AlexaFluor647 (red). (*C*) Anti-C1q levels of selected healthy donors and SLE patient sera (open circles represent donors from whom anti-C1q mAbs were successfully isolated). The dotted line marks cut-off for positivity according to the manufacturer of the kit (QUANTA Lite Anti-C1q ELISA; Werfen). (*D*) Dose–response for recombinant mAb–biotin for binding to C1q assessed in homemade C1q-coated ELISA, detected with streptavidin-HRP. (*E*) Binding of 2 μg/mL anti-C1q mAb to well-known ligands of polyreactive mAbs, chimeric anti-DNP IgG1 (clone G2a2) was used as control mAb. For panels (*D*) and *E*, a representative of at least two independent experiments was shown.

Table 1. Genetic characteristics of human anti-C1q mAbs as analyzed by IMGT V-quest (21)

Heavy Chain

Clone name	Donor	V-gene	V-gene mutations	V-gene identity (%)	D-gene	J-gene	CDR3 AA sequence
2D2	1	IGHV3-74*03 F	14	95.14	IGHD6-13*01 F	IGHJ6*02 F	ARGPHISSWFSDYSYAMDV
1F4	2	IGHV3-30*01 F	37	87.2	IGHD3-16*01 F	IGHJ4*02 F	ARGDCGDVTCSLDS
4C11	2	IGHV1-8*01 F	3	99.0	IGHD3-3*01 F	IGHJ6*02 F	AKISAIFGVVQSGYYYYGMDV
4D2	2	IGHV1-18*01 F	37	87.2	IGHD3-22*01 F	IGHJ3*01 F	ARVNNANFYDRNGYFEGRTR-TEAFDF
4E6	2	IGHV1-18*01 F	35	87.9	IGHD3-22*01 F	IGHJ3*01 F	ARVNNADYYDSSGYFQGRTR-TEAFDF
4F5	2	IGHV4-34*01 F	10	96.5	IGHD3-22*01 F	IGHJ6*02 F	ARERGGHYYEDIGYYGDPGMDV
1F5	3	IGHV1-18*01 F	34	88.2	IGHD6-6*01 F	IGHJ4*02 F	SINSQLAY
3C3	4	IGHV4-39*01 F	16	94.5	IGHD4-17*01 F	IGHJ4*02 F	ASQRDHGDYVRGPDY
12F6	4	IGHV3-21*02 F	1	99.7	IGHD1-26*01 F	IGHJ3*02 F	ARISLVEWELAGYDAFDI

Light Chain

Clone name	Donor	V-gene	V-gene mutations	V-gene identity (%)	kappa/lambda	J-gene	CDR3 AA sequence
2D2	1	IGKV2-28*01 F	3	99.0	kappa	IGKJ1*01 F	MQALQTPPA
1F4	2	IGLV2-11*01 F	23	92.0	lambda	IGLJ1*01 F	CSYGDRNPFV
4C11	2	IGKV2-28*01 F	4	98.6	kappa	IGKJ1*01 F	MQALQTPKT
4D2	2	IGLV2-14*01 F	14	95.1	lambda	IGLJ1*01 F	SSYSSLSPCV
4E6	2	IGLV2-14*01 F	18	93.8	lambda	IGLJ1*01 F	SSYTSLTPCV
4F5	2	IGKV3-20*01 F	8	97.2	kappa	IGKJ4*01 F	QQYGSSPRN
1F5	3	IGKV2-30*01 F	15	94.9	kappa	IGKJ1*01 F	MQGTHWPRT
3C3	4	IGLV1-40*01 F	13	95.5	lambda	IGLJ2*01 F	QSYDSNLSVV
12F6	4	IGLV1-47*01 F	0	100	lambda	IGLJ2*01 F	AAWDDSLSGVV

CDR3, Complementarity-Determining Region 3; AA, amino acid.

targets of (polyreactive) autoantibodies was tested in ELISA. For all anti-C1q mAbs, no binding to single-stranded DNA, lipopolysaccharide (LPS), insulin, or BSA was observed, indicating specificity of these mAbs to C1q (Fig. 1*E*). The avidity of isolated mAbs to C1q was quantified by surface plasmon resonance (SPR). Using solid-phase C1q on the chip and flowing the antibodies in fluid-phase, we observed a strong avidity with K_D values of 6 to 23 nM (Table 2).

Human Monoclonal Anti-C1q Autoantibodies Bind Selectively to Solid-phase C1q. As anti-C1q autoantibodies detectable in the serum of healthy individuals and autoimmune patients are hypothesized to be specific for solid-phase C1q, binding of mAbs to coated, solid-phase C1q in the absence or presence of fluid-phase C1q was analyzed by ELISA. Use of 20 μg/mL purified C1q as a competitor did not yield any notable inhibition of mAbs binding to solid-phase C1q (Fig. 2*A*). Adding normal, C1q-containing, serum also did not result in inhibition for the majority of mAbs. Only four of the mAbs, most notably mAb 4F5, were partially inhibited by C1q in serum at high (25%) concentration (Fig. 2 *B* and *C*). Neither the full $C1qr_2s_2$ complex (denoted C1 hereafter), nor C1q-depleted serum inhibited binding of the anti-C1q mAbs (Fig. 2*D*). Mouse mAb 4A4B11, which is not specific for solid-phase C1q, was strongly inhibited by fluid-phase C1q as expected.

Finally, we studied the preferential binding of anti-C1q mAbs to solid-phase C1q in detail, without potential interference of bivalent binding or Fc-mediated C1q interactions. For this purpose, we engineered antibodies for mAbs 1F4, 1F5, and 4F5 with an Fc domain with mutations that abrogate C1q binding and that contain only a single C1q-binding Fab arm. In ELISA, binding of these anti-C1q mAbs to coated solid-phase C1q was analyzed in the presence of equal amounts of either fluid-phase C1q or C1q on beads (solid-phase). Binding for all three mAbs was significantly inhibited only by C1q on beads, but importantly not by fluid-phase C1q or by human albumin on beads or in fluid-phase (Fig. 2*E*). Altogether, these anti-C1q mAbs show a strong selectivity toward binding to solid-phase C1q.

Human Anti-C1q mAbs Recognize C1q Bound to a Range of Its Natural Ligands. Next, we studied binding of the panel of anti-C1q mAbs to C1q bound to a number of its natural ligands, including IgG, IgM, and CRP, in ELISA (Fig. 3*A*). Binding of anti-C1q mAbs to C1q was detected on all of these ligands, providing evidence that anti-C1q mAbs recognize C1q in its native ligand-bound conformation.

To examine the interaction of anti-C1q mAbs with C1q in a physiologically relevant cellular environment, binding on IgG-opsonized cells and necrotic cells was assessed. Alemtuzumab, a therapeutic anti-CD52 mAb, was chosen for its potent ability to induce classical pathway complement activation. The anti-C1q mAbs indeed exclusively bound to alemtuzumab-opsonized PBMCs in the presence of C1q (Fig. 3*B*). Apoptotic and dead cells are known to be bound by C1q, which improves clearance of these cells by phagocytosis (22). Several anti-C1q mAbs showed binding to C1q on necrotic cells, especially the mAbs with the highest avidity in earlier ELISA experiments, i.e., 1F4, 1F5, and 4F5 (Figs. 1*D* and 3*C*).

Table 2. Avidity of mAbs for C1q as determined by Surface Plasmon Resonance

mAb	K_D (M)	k_a (1/Ms)	k_d (1/s)
1F4	8.1×10^9	1.4×10^5	1.1×10^3
1F5	2.2×10^8	1.1×10^5	2.4×10^3
2D2	2.0×10^8	9.7×10^4	2.0×10^3
3C3	2.0×10^8	6.3×10^4	1.2×10^3
4C11	2.3×10^8	1.8×10^5	4.3×10^3
4D2	2.3×10^8	9.9×10^4	2.3×10^3
4E6	2.1×10^8	1.4×10^5	2.9×10^3
4F5	6.0×10^9	1.4×10^5	8.4×10^4
12F6	2.3×10^8	6.6×10^4	1.5×10^3

On western blot, unheated C1q, was detected by all anti-C1q mAbs, in contrast to heat-treated C1q (both reduced and non-reduced) (*SI Appendix*, Fig. S1). This indicates that the epitopes on C1q also become exposed in immobilized C1q in this context, but are destroyed upon heat denaturation.

Human Anti-C1q Autoantibodies Target Multiple Epitopes on the CLR of C1q. To investigate the C1q domains and epitopes that are targeted by these anti-C1q mAb, binding competition between mAbs was explored in ELISA (Fig. 4*A*). While all anti-C1q mAbs display the expected self-inhibition, each mAb show different levels of inhibition with the other mAbs. Two distinct groups of mAbs could be discerned, competing with each other but not with mAbs from the other group. Both groups consist of mAbs from multiple donors, while each group contains at least one mAbs originating from donor 2, showcasing diversity of targeted epitopes within one individual. These data provide evidence for at least two different epitopes on C1q that are recognized by human anti-C1q autoantibodies.

The binding sites for our anti-C1q mAbs were compared with anti-C1q from SLE patients. To this end, antibodies from serum of three SLE patients (SLE A, B, and C) were purified on protein A, and competition for binding to C1q between mAbs and SLE antibodies was evaluated (Fig. 4*B*). Competition patterns were clearly split between the two groups identified in mAb–mAb competition. Epitopes targeted by SLE A and SLE B overlap with epitopes of mAbs 1F4, 1F5, 3C3, and 12F6, while SLE C antibodies compete with mAbs 2D2, 4C11, 4D2, 4E6, and 4F5. Each anti-C1q mAb was inhibited by the presence of at least one of the polyclonal SLE antibody mixes, showcasing that our anti-C1q mAbs target the same or similar epitopes as anti-C1q autoantibodies in SLE patients.

Additionally, a mixture of mAbs 1F4, 1F5, 4D2, and 4F5 showed near-complete inhibition of anti-C1q binding from purified SLE antibodies (*SI Appendix*, Fig. S2). These data further indicate that in several anti-C1q-positive SLE patients, there is

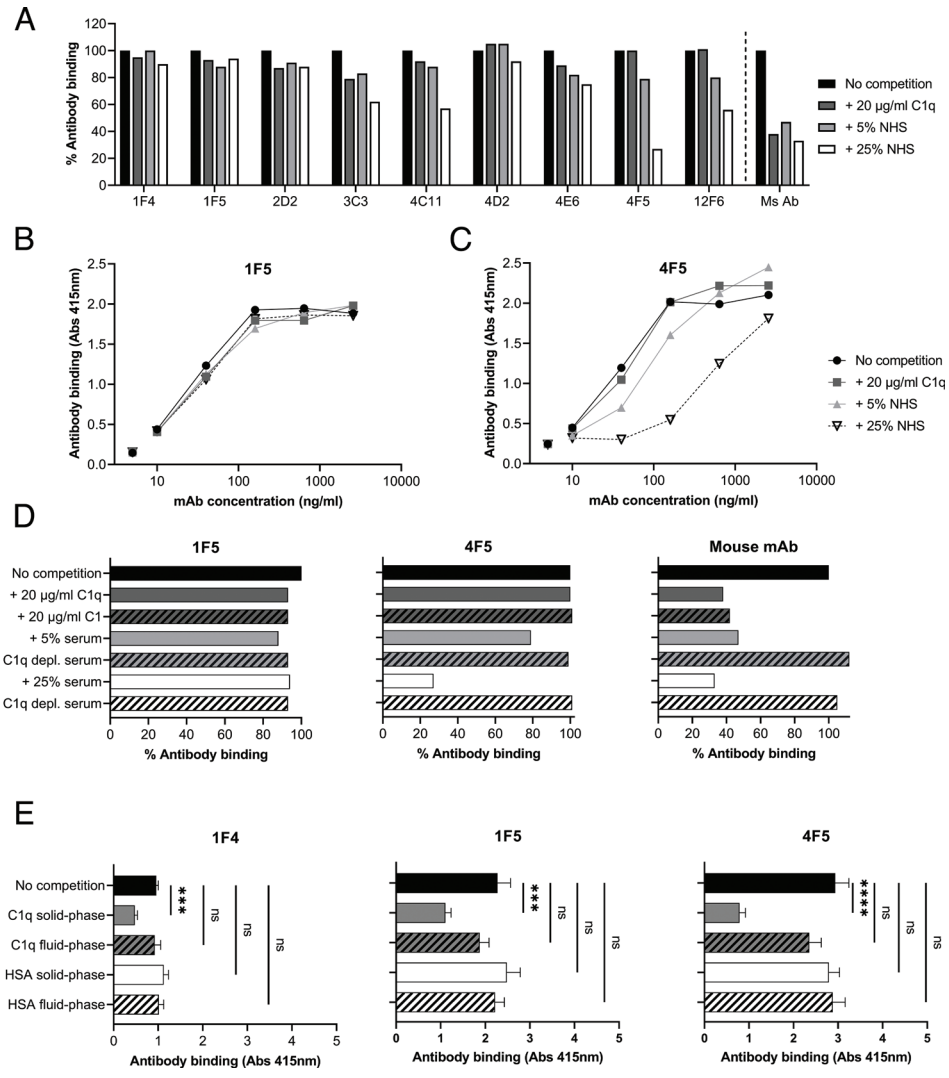

Fig. 2. Binding of anti-C1q mAbs in ELISA in the presence of fluid-phase and solid-phase C1q. (*A*) Fluid-phase C1q competition measured in ELISA for all mAbs at a concentration at the top of the linear range for the specific mAb, to ensure competition could be detected optimally. Mouse mAb 4A4B11, which binds C1q but is not specific for solid-phase C1q, was included as a control. The measurements were performed at mAb concentrations of 160 ng/mL (1F5, 4F5, mouse mAb 4A4B11), 640 ng/mL (3C3, 4D2, 4E6), 2,560 ng/mL (1F4, 2D2, 4C11), or 10,240 ng/mL (12F6). Data shown are representative for two independent experiments. (*B* and *C*) Example titrations of competition assay with fluid phase purified C1q or NHS, for mAbs 1F5 (which shows no competition from high-concentration fluid-phase C1q) and 4F5 (which shows some competition from 25% NHS). (*D*) Competition with fluid-phase purified C1 or C1q, NHS, or C1q-depleted serum for selected anti-C1q mAbs 1F5, 4F5 and mouse mAb 4A4B11. (*E*) Anti-C1q mAb binding (monovalent with inactive Fc domain) to the C1q-coated ELISA plate is inhibited by solid-phase C1q on beads, but not by an equal amount of fluid-phase C1q. Data shown are representative for two independent experiments; bars indicate means and error bars indicate SDs. One-way ANOVA with Dunnett's multiple comparison test, compared to no competition; ns, not significant; *** $P < 0.001$; **** $P < 0.0001$. NHS, normal human serum.

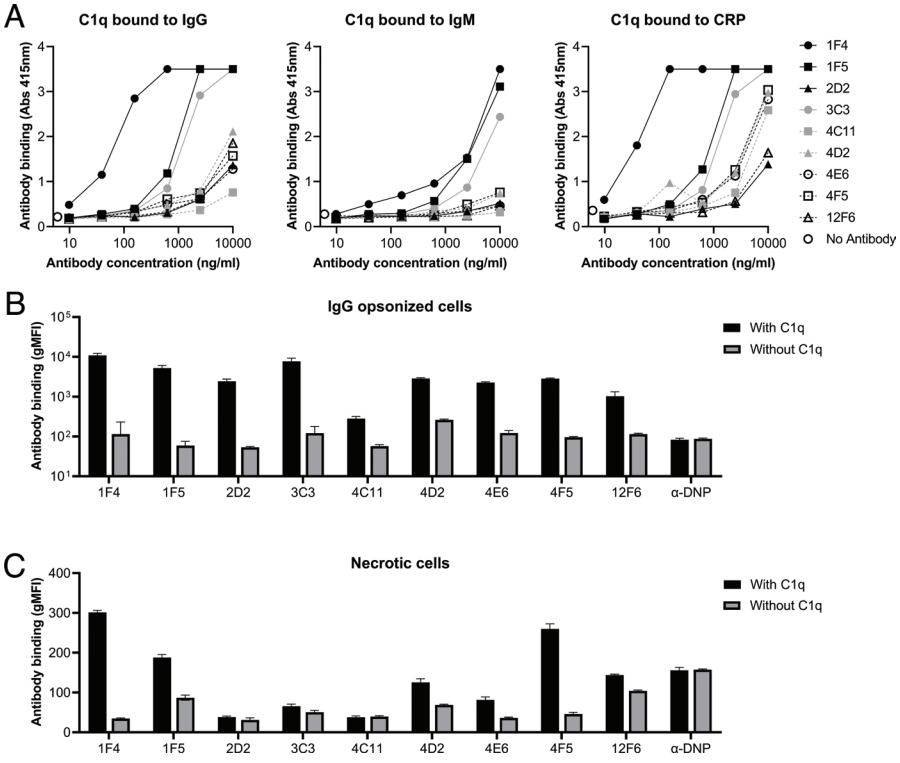

Fig. 3. Binding of human anti-C1q mAbs to C1q on various ligands and surfaces. (*A*) Binding of anti-C1q mAbs to C1q on coated IVIG, IgM, and CRP in ELISA. (*B*) Binding of anti-C1q mAbs to alemtuzumab-opsonized PBMCs in flow cytometry, in the presence and absence of C1q. Anti-DNP was included as a negative control which does not bind C1q. (*C*) Binding of anti-C1q mAbs to necrotic PBMCs in flow cytometry, in the presence and absence of C1q. Anti-DNP was included as a negative control which does not bind C1q. All data shown are representative for at least two independent experiments. In panels (*B* and *C*), the geometric mean of fluorescence intensity (gMFI) and SD of triple measurements is indicated.

no anti-C1q reactivity present which is not covered by the set of anti-C1q mAbs presented in this manuscript.

A screening of linear peptides with a length of 21 amino acids, covering all three chains of the C1q protein, revealed that none of the anti-C1q mAbs recognized a linear peptide (*SI Appendix*, Fig. S3). In order to map the binding of anti-C1q mAbs to the different regions of the C1q molecule, binding to CLR and recombinant GH domain was evaluated (Fig. 4*C*). All anti-C1q mAbs evidently bind to the CLR and not the GH when tested in ELISA, with the exception of mAb 12F6, which only bound to full C1q.

Electron Tomographic Imaging of Anti-C1q Bound to Ig-C1q Complexes. In order to visualize the binding of anti-C1q mAbs to immune complexes with C1q, we used electron tomography. For the electron microscopy studies, a monovalent, Fc-inactive variant of the anti-C1q mAb 1F5 was used to avoid C1q–Fc interaction and bivalent binding. First, anti-C1q mAb binding to C1q–$(IgG)_6$ complexes was visualized using negative stain electron tomography (Fig. 5*A*). C1q–$(IgG)_6$ complexes could be directly interpreted in the tomographic slices. However, since the anti-C1q antibodies bound to more than one binding site per complex and the whole complex is highly flexible, it was not straightforward to visualize anti-C1q antibody molecules directly. As a metric to determine where anti-C1q IgG were located, we masked a circular region of 26 nm, corresponding to the approximate diameter of the C1q–$(IgG)_6$ complex, and any additional density bound to, but outside of, this region was interpreted as an anti-C1q mAb (Fig. 5*B*). These data were used to build molecular models of the C1q–$(IgG)_6$–anti-C1q complexes, which could be overlaid with the tomographic slices to aid interpretation (Fig. 5*C*).

We observed multiple anti-C1q antibodies bound per complex, located at the periphery of the C1q–$(IgG)_6$ complex. These observations demonstrate the presence of multiple epitopes of a monoclonal autoantibody on each C1q protein. Interestingly, although anti-C1q mAbs recognize an epitope in the CLR of C1q, we could observe that they bind in close proximity to the GH domains and not, as hypothesized beforehand, to the top stalk of the C1q molecule. These structural data provide important insights into the molecular interaction between C1q and C1q autoantibodies.

Anti-C1q mAbs Increase Fc-receptor Engagement, but Not Complement Activation, on Immune Complexes. We sought to understand the consequences of the presence of anit-C1q autoantibodies on the activation of the immune system by C1q-containing immune complexes. When anti-C1q binds to C1q on an immune complex, its Fc domain may add to the immune response by increasing complement activation or by Fc-receptor engagement and cell-mediated effector functions. Plate-bound IgG complexes allow classical pathway complement activation, in this case detected by C5b9 deposition with increasing serum concentration between 0.5% and 4% normal human serum (NHS) (Fig. 6*A*). From this titration, we selected 1% NHS as a source of serum to further analyze whether the presence of anti-C1q mAbs would impact on the degree of complement activation. The presence of anti-C1q mAbs did not or only slightly increase complement activation, and in the case of two of the mAbs, a significant decrease of C5b9 generation was observed (Fig. 6*B*).

When investigating Fc-receptor binding in the same context, deposited IgG complexes interacted with FcγRIIIa. Importantly, when C1q was present on the hexameric IgG, the binding of FcγRIIIa is highly impaired (Fig. 6*C*). From the titration, we chose 3 μg/mL of FcγRIIIa to analyze the impact of anti-C1q mAbs. We observed that several anti-C1q mAbs were able to increase FcγRIIIa binding on C1q-containing immune complexes by 20% to 60% (Fig. 6*D*). Interestingly, anti-C1q mAbs 3C3 and 4F5 show the highest FcγRIIIa binding, while also causing a decrease in complement activation of immune complexes. Focusing on functional consequences of Fc-receptor binding by anti-C1q mAbs, we investigated binding of IgM-coated beads opsonized with C1q by THP-1 cells differentiated toward macrophages. In this setting, the binding of IgM-coated/C1q opsonized beads is minimal, but addition of 1 μg/mL anti-C1q mAb increased binding of the beads to the differentiated THP-1 cells as much as fivefold (Fig. 6*E*). When Fc receptors of cells are partially blocked

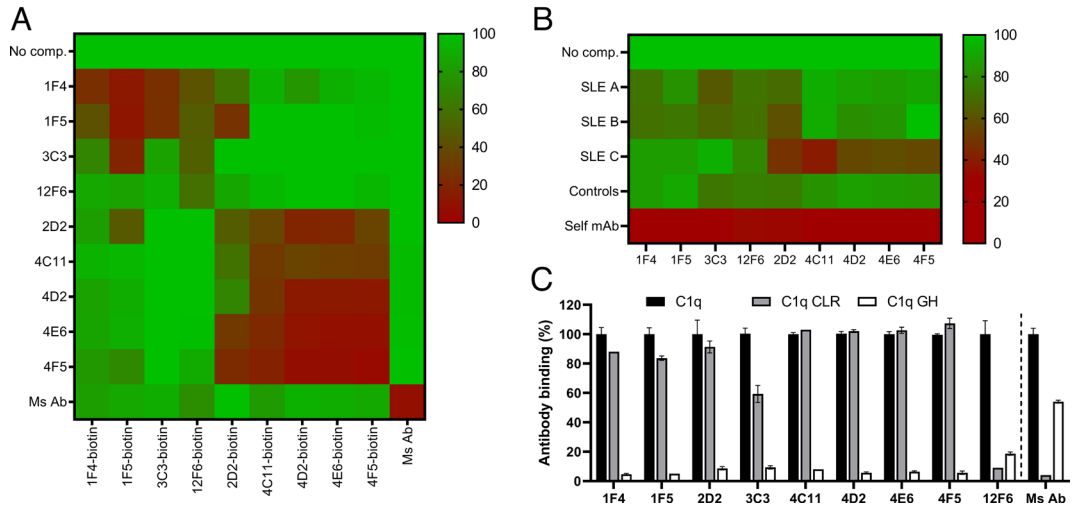

Fig. 4. Determination of C1q epitope targeted by human anti-C1q mAbs. (*A*) Competition for binding to C1q-coated ELISA, between human anti-C1q mAbs, and with unrelated mouse anti-C1q mAb 4A4B11. The average percentage residual signal compared to no competition from two independent experiments is indicated in the heatmap. (*B*) Competition for binding to C1q-coated ELISA, between biotinylated anti-C1q mAbs and polyclonal anti-C1q antibodies from SLE serum, the percentage residual signal compared to no competition is indicated in the heatmap. Data are representative of two independent experiments. (*C*) Anti-C1q mAb binding to full C1q, C1q collagen-like region (C1q CLR), and C1q (recombinant) globular head (C1q GH) domains in ELISA; signal is normalized to 100% for binding to full C1q; mean and SD are shown. Ms Ab is mouse mAb 4A4B11; data shown are representative for three independent experiments.

by pre-incubating with an Fc receptor blocking agent, inhibition of binding of opsonized beads is observed, confirming that this is an Fc receptor–driven process (Fig. 6*F*). In a similar fashion, we studied whether anti-C1q mAbs could enhance phagocytosis of bacteria by human neutrophils. *S. aureus* was labeled with a monoclonal antibody targeting wall teichoic acid (WTA, an *S. aureus* surface glycopolymer (23). Specifically, we used anti-WTA IgG4 because this isotype does not drive Fc-receptor-mediated phagocytosis directly but can interact with C1q after introduction of hexamer-enhancing mutations (24). Anti-C1q mAbs were able to enhance phagocytosis of bacteria to various degrees after opsonization with an antibody isotype that does not facilitate phagocytosis (Fig. 6*G*). Anti-C1q mAbs thus do not notably enhance complement activation but highly enhance the capacity both IgM- and IgG-opsonized and C1q-containing immune complexes to engage Fc receptors and induce effector function.

Discussion

In the current study, we investigated the characteristics and functional properties of human anti-C1q autoantibodies on a monoclonal level. Autoantibodies against C1q are present in several

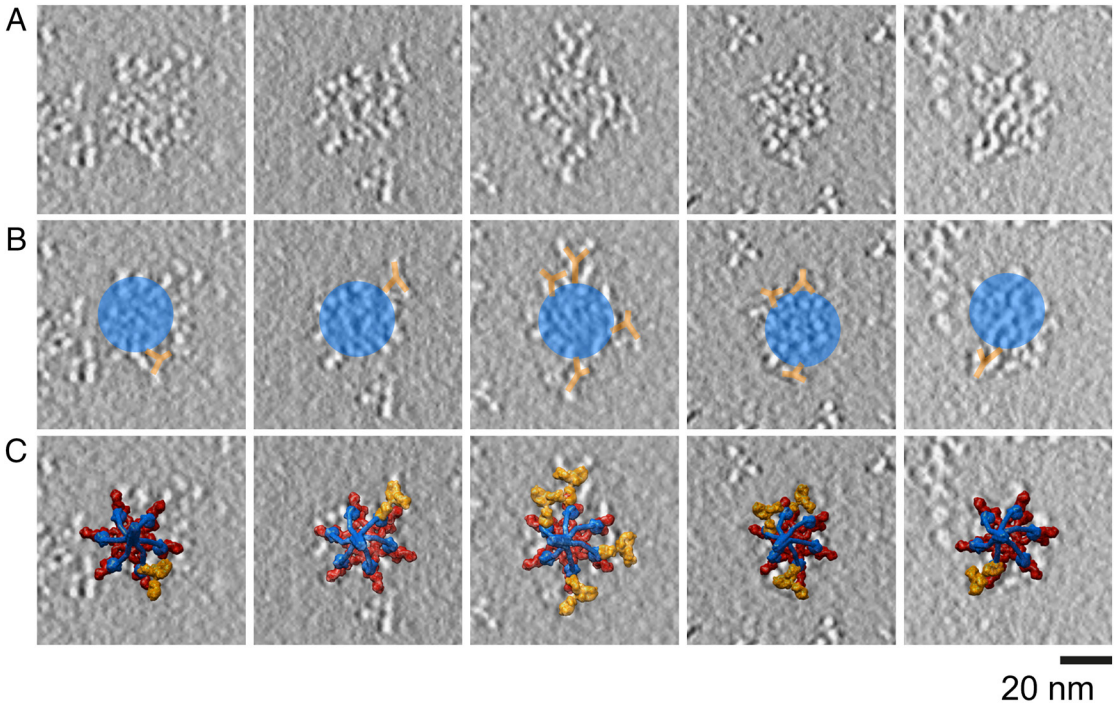

Fig. 5. Electron tomography images of C1q bound by anti-C1q mAb. (*A*) 4.5-nm thick negative stain electron tomogram slices of hexameric anti-CD52 IgG-RGY, C1q, and monovalent, Fc-inactive anti-C1q mAb 1F5. (*B*) Overlay indicating the complex of hexameric IgG and C1q (blue area) and proposed location of anti-C1q mAb (yellow). (*C*) Overlay indicating the IgG (red), C1q (blue), and anti-C1q mAb (yellow) complex model on top of negative stain tomographic slices for better visualization (Scale bar, 20 nm).

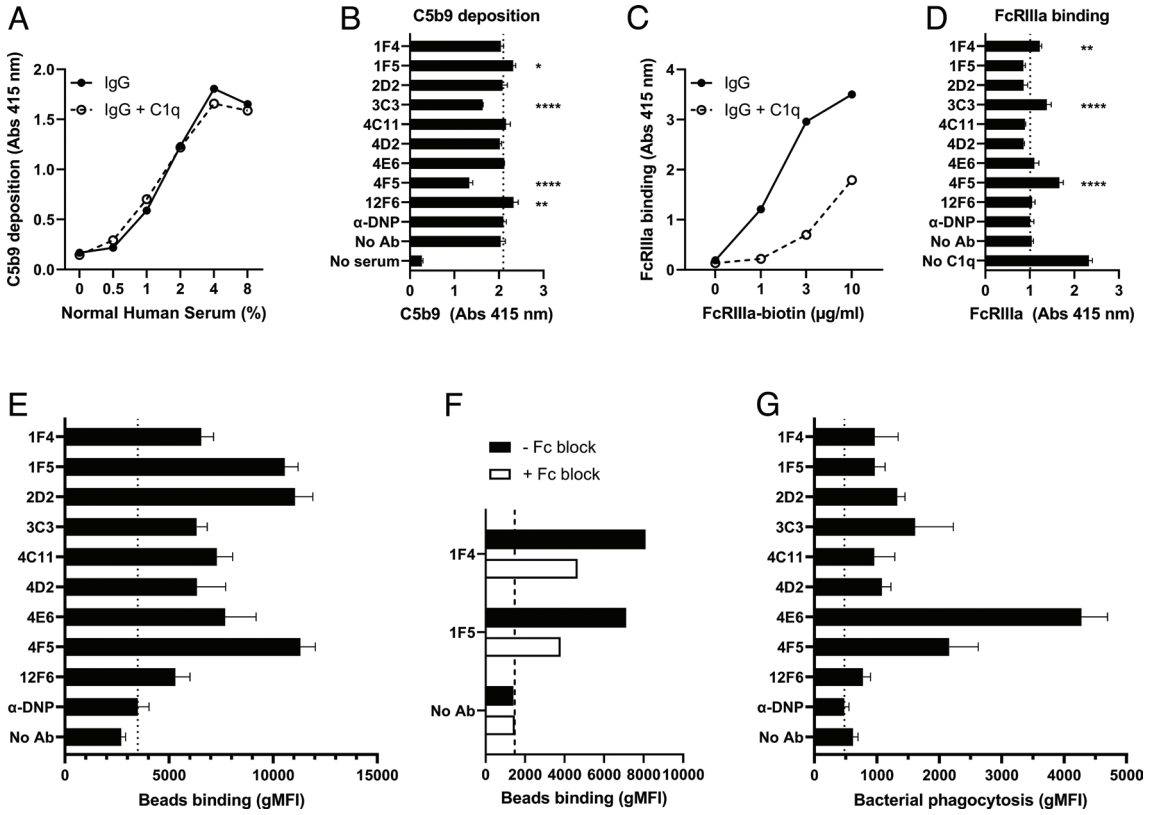

Fig. 6. Anti-C1q mAbs stimulate Fc receptor engagement and phagocytosis, but not complement activation. (*A*) Complement activation on hexameric IgG complexes with or without extra C1q in ELISA was detected on the level of C5b9. On the basis of the NHS titration, we selected 1% NHS for the following experiment to investigate the effect of anti-C1q mAbs. (*B*) C5b9 deposition on hexameric IgG complexes in ELISA, in the presence of different anti-C1q mAbs at 1% NHS. (*C*) Binding of biotinylated FcγRIIIa to hexameric IgG complexes with or without extra C1q in ELISA, on the basis of the FcγRIIIa titration, we used 3 µg/mL FcγRIIIa in the following experiment to investigate the effect of anti-C1q mAbs. (*D*) FcγRIIIa-biotin binds to hexameric IgG complexes and different anti-C1q mAbs in ELISA. (*E*) PMA-differentiated THP-1 cells bind IgM-coated/C1q-opsonized beads, in the presence of anti-C1q mAbs. (*F*) PMA-differentiated THP-1 cell interaction with IgM-coated/C1q-opsonized beads is inhibited by an Fc-blocking agent. (*G*) Human neutrophils phagocytose *Staphylococcus aureus* bacteria opsonized with anti-WTA IgG4-E430G and C1q, in the presence of anti-C1q mAbs. For *B* and *D–F*, mean and SD are shown; data are representative for three experiments. For (*B* and *D*), each anti-C1q mAb was compared to anti-DNP with one-way ANOVA followed by Dunnett's multiple comparisons test. * $P < 0.05$; ** $P < 0.01$; *** $P < 0.001$; **** $P < 0.0001$.

diseases such as SLE and HUVS but also in a substantial number of healthy individuals (5, 6). In SLE, the presence of anti-C1q autoantibodies is associated with the development of lupus nephritis (9). Experimental studies indicate that anti-C1q autoantibodies contribute to renal disease only when there are C1q-containing immune complexes in the glomeruli (7). In this study, we have obtained a set of anti-C1q mAbs from healthy individuals and confirmed that these antibodies have a similar binding profile as anti-C1q autoantibodies in SLE patients. The information obtained from the analysis of the molecular properties of these anti-C1q autoantibodies sheds light on a role of anti-C1q in healthy individuals as well as on a role for these antibodies in pathological conditions such as lupus nephritis. Importantly, the molecular properties of these anti-C1q autoantibodies may allow the development of specific therapeutic or diagnostic tools.

We have obtained nine anti-C1q mAb, all derived from healthy individuals. Our attempts to isolate anti-C1q-producing B cell clones from SLE patients were not successful, possibly due to the immunosuppressive treatment that the patients received. To confirm that the analysis of anti-C1q mAbs isolated from healthy donors is meaningful for the understanding of anti-C1q antibodies in SLE, we performed competition experiments using purified IgG of anti-C1q-positive SLE patients. This confirmed that the anti-C1q mAbs isolated from healthy donors indeed all target C1q epitopes that are also targeted by anti-C1q autoantibodies present in SLE patients, underscoring the relevance of the identified anti-C1q mAbs. By isolating only anti-C1q of the IgG isotype and producing it recombinantly in IgG1 subclass, some information on the presence of various isotypes and subclasses may have been lost. However, IgG is evidently the dominant isotype among anti-C1q autoantibodies in SLE patients, while the subclasses IgG1, IgG2, and IgG3 are all regularly found (25, 26).

All anti-C1q clones were first identified using ELISA with anti-IgG detection and amplified with primers specific for IgG. Therefore, the B cells producing these anti-C1q in vivo must have undergone class-switching to IgG. In B cells, class-switching and avidity maturation often occur at the same developmental stage. Indeed, we observed high avidity of anti-C1q for its antigen in SPR experiments. The range of binding strengths observed in ELISA and cellular assays was not fully mirrored in the SPR results, where less variation in avidity was detected. These differences may be explained by the different manner of presenting solid-phase C1q or by the fundamental difference in techniques, as ELISA requires interactions to resist multiple washing and incubation steps to be registered, whereas SPR does not and consequently measures more native-like interactions. These steps in ELISA and cellular assays may work to amplify any differences in binding strength (27). Interestingly, class-switching and avidity maturation are both processes that only commence in B cells if there is sufficient T cell help, indicating that in SLE patients and in healthy controls, T cell help for C1q-reactive B cells must be present. Currently, there are no studies into the nature of the T cell help. This would be highly interesting as the B cells are reactive to a conformational epitope and the T cells will be

reactive to a linear peptide presented in human leukocyte antigen (HLA); this may be a C1q peptide or a peptide from any protein in the C1q-containing immune complex.

In determining the epitope targeted by anti-C1q mAbs, we could classify our anti-C1q mAbs in two groups based on competition assays. All but one anti-C1q mAb bound to C1q CLR almost as strong as to full C1q. The binding to C1q CLR is in accordance with earlier studies on anti-C1q-antibody-positive sera (28). The presented slices through electron tomographic volumes indicate binding of anti-C1q mAb 1F5 to an epitope on the CLR close to the GH domain of C1q. While no exact epitope could be determined, this experiment contributes to identifying one of the regions of C1q targeted by human anti-C1q autoantibodies. The location of antibody binding and the observation that multiple anti-C1q 1F5 mAbs can bind to one C1q molecule also indicate that the target epitope is likely present on the extended arms of the C1q CLR and not on the central CLR stalk where all arms come together. This may be explained by the GH domains bending at the interface of CLR and GH upon docking onto a ligand (29, 30), revealing a cryptic binding site previously obscured when in fluid phase. Collectively, the data indicate that anti-C1q mAbs bind C1q in a conformationally changed state, which occurs in C1q following binding to its natural ligands, or to surfaces (Fig. 7 *A*–*C*).

While the origin of anti-C1q autoantibody reactivity is still unclear, there may be some benefit to the host under certain conditions, once these antibodies have arisen. We hypothesized that anti-C1q antibodies of the IgG isotype could aid in phagocytosis of C1q-opsonized particles by engaging Fc receptors. Indeed, addition of anti-C1q mAbs increased binding and phagocytosis of opsonized beads and *S. aureus* bacteria. In vivo, the same mechanism could enhance the clearance of C1q-opsonized pathogens and apoptotic cells.

Nonetheless, the presence of anti-C1q autoantibodies in SLE patients is heavily linked to nephritis (7–9), likely because of the additional immune activation on C1q-containing immune complexes deposited in the glomeruli. In a mouse model of anti-C1q enhancement of immune-complex nephritis, we observed earlier that both complement activation and Fc receptor engagement were necessary for kidney damage (7). Based on the current findings, we now hypothesize that complement activation by the immune complexes in the kidney is required to attract inflammatory cells to the glomerulus but is not enhanced by anti-C1q autoantibodies. The anti-C1q driven Fc-receptor triggering would then mediate damage to the kidneys by the newly attracted immune cells. Future research using in vivo experiments in mice would be needed to further support this hypothesis. Unfortunately, such an experiment is currently not possible, as these human anti-C1q mAbs bind strongly to human C1q, but do not bind substantially to mouse C1q.

In our experiments, anti-C1q mAb binding to solid-phase C1q was not, or only marginally, inhibited by fluid-phase C1q. Reversely, anti-C1q mAb binding could be inhibited in the same assay with solid-phase C1q on beads, re-iterating the specificity of these antibodies. The specific targeting of solid-phase C1q could potentially be used diagnostically or therapeutically. In a diagnostic setting, the isolated anti-C1q mAbs may be used to identify tissue locations where C1q is activated in vivo. Therapeutically, anti-C1q mAbs may be exploited in approaches to enhance or decrease C1q-immune complex-mediated effects.

The current study reveals molecular properties of human anti-C1q autoantibodies on a monoclonal level. These autoantibodies bind specifically to solid-phase C1q, which exposes cryptic epitopes not available in fluid-phase C1q. The data provide insights into the immunopathological processes that underlie lupus nephritis and may therefore be an important step in fighting this autoimmune disease.

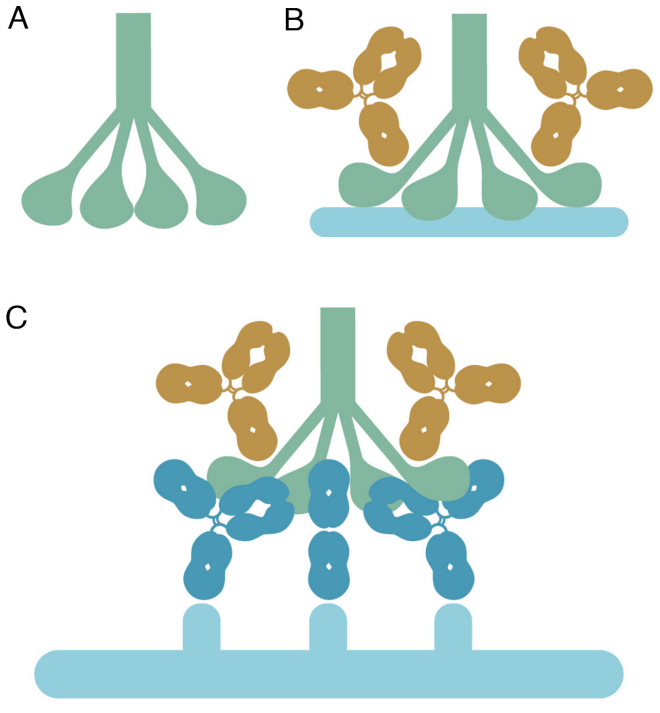

Fig. 7. Schematic overview of binding of anti-C1q to solid-phase C1q. (*A*) Fluid-phase C1q is not bound by human anti-C1q autoantibodies. (*B* and *C*) When C1q binds to a (cell) surface (*B*) or ligand such as IgG complex (*C*), it adopts a solid-phase conformation. This conformation reveals a previously hidden epitope, targeted by anti-C1q autoantibodies, allowing them to specifically bind to solid-phase C1q.

Materials and Methods

ELISA to Screen Individuals for Anti-C1q-antibody Positivity. Serum of selected individuals was screened for the presence of anti-C1q antibodies by QUANTA Lite Anti-C1q (Werfen) enzyme-linked immunosorbent assay (ELISA) according to the manufacturer's protocol (Werfen). Briefly, samples were diluted 1:101 in Sample Diluent and 100 µL diluted samples or supplied controls were added to the wells. After 30-min incubation, wells were washed and incubated with 100 µL horseradish peroxidase (HRP) IgG conjugate for another 30 min. Next, wells were washed and stained for 30 min with 100 µL 3,3′,5,5′-tetramethylbenzidine (TMB) Chromogen while protected from light; then, 100 µL HRP Stop Solution was added. Absorbance at 450 nm was measured with a microplate reader (Bio-Rad iMark) and used to calculate anti-C1q units based on positive control samples provided in the kit. The cut-off for positivity was 20 units, as recommended by the manufacturer.

Isolation of C1q-reactive B Cells. To optimize the anti-C1q staining procedure, HEK cells were transduced to express mouse anti-C1q mAb JL-1 on the cell surface, as described before (7, 31). The resulting cells mimic B cells with a C1q-binding B cell receptor. For fluorescence-activated cell sorting (FACS) of B cells, peripheral blood was collected from anti-C1q-positive donors after obtaining their informed consent, approval was granted by the Medical Ethical Committee of Leiden-The Hague-Delft (reference numbers: B19.008/AB/ab and P17.151). Peripheral blood mononuclear cells (PBMC) were isolated using Ficoll-Paque (Leiden University Medical Center [LUMC] pharmacy) gradient centrifugation and B cells were enriched using the EasySep Human B cell isolation kit (Stem Cell Technologies) following instructions provided by the manufacturer. Fluorescent solid-phase C1q-containing complexes were generated by mixing purified C1q (Complement Technologies), pre-formed hexamers of anti-dinitrophenol (DNP) IgG1-RGY antibodies, biotinylated peptides containing DNP (LUMC peptide facility) and streptavidin-phycoerythrin (PE) (Bio Rad) or streptavidin-AlexaFluor647 (Invitrogen) (Fig. 1*B*). IgG1 antibodies (mAb G2a-2) directed against the hapten DNP (32) were engineered with hexamerization-enhancing mutations E345R, E430G, and S440Y to generate hexamers of IgG that bind C1q, thereby bringing it

in its solid-phase conformation (30, 33). The anti-DNP antibodies bind a peptide containing DNP and biotin, linking it to the streptavidin-coupled fluorochromes.

B cells were incubated with fluorescent solid-phase C1q complexes for 45 min at 4 °C. After washing in phosphate-buffered saline (PBS) with 1% fetal calf serum (FCS), the cells were further stained with mouse anti-human CD27-FITC (ThermoFisher; mAb CLB-27/1), CD3-Pacific Blue (BD Biosciences; mAb SP34-2) and IgD-PE-Cy7 (BD Biosciences, mAb IA6-2) and incubated for 45 min at 4 °C (34). Single B cells detected as $CD3^-$, IgD^-, $CD27^+$, and double positive for C1q-complex staining were sorted on a FACSAria III Cell Sorter (BD Biosciences) and collected at one cell per well in a 96-well flat bottom plate (Corning). The wells contained 100,000 irradiated (50 Gy) EL4B5 cells (35) expressing CD40L in 200 μL Iscove's Modified Dulbecco's Medium (IMDM; Lonza) supplemented with 10% FCS, 2 mM L-glutamine (Gibco), 50 μM 2-mercaptoethanol (Sigma-Aldrich), 100 units/mL penicillin, 100 μg/mL streptomycin (both Gibco), 20 μg/mL Insulin-transferrin-sodium selenite (Sigma-Aldrich), 50 ng/mL interleukin (IL)-21 (Gibco), 1 ng/mL IL-1β (Miltenyi Biotec), 0.3 ng/mL tumor necrosis factor (TNF)-alpha (Miltenyi Biotec), and 0.5 μg/mL Resiquimod (R848; Sigma-Aldrich) (36). Plates with B cells were incubated for 13 d at 37 °C and 5% CO_2 before analysis.

Identification and Variable Domain Sequence Analysis of Anti-C1q-producing B Cells. Supernatant of sorted B cells was harvested after a 13-d expansion period and screened for IgG production by ELISA as described before (37). Screening for C1q reactivity in the B cell supernatant was performed by coating C1q instead of goat anti-human-IgG. B cell clones which were positive for anti-C1q production were lysed and RNA was isolated using TRIzol reagent (Invitrogen). Subsequently, cDNA was synthesized using PrimeScript Reverse Transcriptase (Takara) followed by rapid amplification of cDNA ends (RACE) PCR to amplify variable domains of the heavy (VH) and kappa or lambda light (VL) chain. Isolated VH and VL fragments were ligase-independently cloned into pcDNA3.3 plasmids containing IgG1, kappa or lambda constant domains, as described before (38). The plasmids were then sequenced by the Leiden Genome Technology Center to obtain the VH and VL sequences. Sequences were analyzed for VDJ gene usage and complementarity-determining region (CDR) identification by IMGT V-quest (39).

Production and Purification of Monoclonal Antibodies. Heavy and light chain plasmids were co-transfected in Expi293F cells using ExpiFectamine, Opti-MEM, and Expi293 expression medium (all ThermoFisher) according to the manufacturer's instructions. Supernatant was harvested after 5–7 d and filtered, and antibodies were purified on protein A resin (Genscript). Subsequently, buffer was exchanged to PBS, and antibodies were concentrated on 50 kDa Amicon centrifugal filters (Merck Millipore). Antibody concentration was measured using an in-house sandwich ELISA as described previously (37).

ELISA for Binding of Anti-C1q mAbs to C1q on Natural Ligands and Polyreactivity. ELISA was performed to evaluate reactivity of the isolated mAbs toward C1q on natural ligands and toward common targets of polyreactive antibodies. Nunc MaxiSorp plates (ThermoFisher) were coated with 10 μg/mL calf thymus single-stranded DNA (Sigma-Aldrich), lipopolysaccharide (LPS; Sigma-Aldrich), pre-pro-insulin (produced in-house), intravenous immunoglobulins (IVIG; Sanquin), CRP (Calbiochem), 5 μg/mL IgM (Sigma-Aldrich) or 5 μg/mL C1q in bicarbonate coating buffer (0.1 M Na_2CO_3/$NaHCO_3$, at pH 9.6) for 1 h at 37 °C. Plates were washed three times with PBS/0.05% Tween after every incubation. Plates were blocked with 100 μL/well PBS/1% bovine serum albumin (BSA) for 1 h at 37 °C. Wells coated with IVIG, IgM, or CRP were incubated with 5 μg/mL C1q diluted in PBS/0.05% Tween/1% BSA (hereafter abbreviated to PTB) for 1 h at 37 °C. After washing, plates were incubated with anti-C1q mAbs biotinylated with the Pierce Antibody Biotinylation Kit (ThermoFisher) diluted in PTB and incubated for 1 h at 37 °C. Binding of anti-C1q mAbs was detected by 0.5 μg/mL HRP-coupled streptavidin (ThermoFisher) in PTB, incubated for 1 h at 37 °C. After the final washing sequence, 50 μL 2,2′-azino-bis(3-ethylbenzothiazoline-6-sulfonic acid) (ABTS)/0.015% H_2O_2 (both from Merck) was added, and absorbance at 415 nm was measured using a microplate reader.

Avidity Measurement of Anti-C1q mAbs by Surface Plasmon Resonance. Surface plasmon resonance (SPR) was employed to determine the avidity of anti-C1q mAbs for C1q, using a Biacore T200 (Cytiva). Biotinylated C1q was immobilized on a streptavidin-coated chip (Cytiva) to a response of 146.4 response units, with an empty channel for compensation. By immobilizing C1q on the chip, it was presented in solid-phase. Next, titration curves of anti-C1q mAbs or unrelated mouse anti-C1q mAb 4A4B11 (ATCC HB-8327) in PBS/0.05% Tween/0.5 mg/mL BSA from 40 to 0.05 μg/mL were prepared. These samples were stored in the Biacore at 4 °C and covered with a breakable seal during the measurement to ensure a stable quality of the samples. Samples were run in increasing concentration steps, with chip regeneration by two times 30 s flowing 10 mM glycine, pH = 2.0. Resulting binding curves were analyzed using Biacore T200 Evaluation Software 3.2.1 (Cytiva) to fit a 1:1 binding model, resulting in association and dissociation constants for each anti-C1q mAbs.

ELISA to Determine Inhibition of Anti-C1q mAbs by Fluid Phase C1q. ELISA plates were coated with 10 μg/mL C1q in coating buffer overnight at 4 °C and subsequently blocked with PBS/1%BSA for 1 h at 37 °C. Biotinylated anti-C1q mAbs were mixed with either 20 μg/mL C1q, 20 μg/mL C1 (Complement Technologies), 5% or 25% pooled normal human serum (NHS) or 5% or 25% C1q-depleted serum (Complement Technologies), in PTB containing 0.5 M NaCl to prevent C1q–Fc interactions (13). Mouse mAb 4A4B11 was tested as a control which is not specific for solid-phase C1q. Samples with serum were also supplemented with 10 mM EDTA to prevent complement activation. After pre-incubation on ice for 30 min, samples were incubated in the C1q-coated wells for 1 h at 37 °C. Anti-C1q mAbs were detected with 0.5 μg/mL streptavidin-HRP, plates were then developed by incubating with ABTS/0.015% H_2O_2 and measured using a microplate reader. Percentage signal was calculated by setting the absorbance values of samples without C1q competition at 100% for each individual mAb.

ELISA to Determine Inhibition of Monovalent Anti-C1q mAbs by Solid-phase C1q. For mAbs 1F4, 1F5, and 4F5, antibody was produced containing LALA-PG mutations to render their Fc domain incapable of recruiting C1q [LALA-PG (40) and F405L or K409R mutations to allow for Fab-arm exchange. These antibodies were then combined with the anti-HIV gp120 clone b12 through Fab-arm exchange following the protocol described by Labrijn et al. (41). The resulting bispecific antibodies (bsAb) were functionally monovalent for C1q binding, with inactive Fc domains to specifically investigate the interactions between one C1q molecule and one antigen binding domain. ELISA plates were coated with 10 μg/mL C1q in coating buffer overnight at 4 °C and subsequently blocked with PBS/1%BSA for 1 h at 37 °C. Biotinylated anti-C1q bsAb in PTB were mixed with C1q or human serum albumin (HSA) coupled to Carboxyl Fluorescent Particles, 0.4–0.6 μm (Spherotech), or soluble C1q or HSA. After pre-incubating for 30 min, each well in the ELISA plate received 0.1 μg anti-C1q antibody and 1 μg C1q or HSA, which in case of solid-phase competition was coupled to 10^9 beads. After incubating for 1 h at 37 °C, plates were washed and bound, biotin-labeled anti-C1q antibodies were detected with 0.5 μg/mL streptavidin-HRP. Plates were developed by incubating with ABTS/0.015% H_2O_2 and measured using a microplate reader.

Anti-C1q mAbs Binding to C1q on Opsonized and Necrotic Cells. PBMCs were isolated from healthy donor peripheral blood by Ficoll-Paque gradient centrifugation. Cells were either opsonized with recombinant anti-CD52 (alemtuzumab) IgG1 antibodies containing hexamer-enhancing mutations RGY (42) for 45 min at 4 °C or made necrotic by incubating for 30 min at 56 °C (43). Cells were then seeded into 96-well plates at 100,000 cells per well and washed two times by adding 200 μL FACS buffer (PBS/2% FCS), centrifuging and removing the supernatant. C1q was added at 2 μg/mL in FACS buffer and incubated with the cells for 45 min at 4 °C. After washing, cells were incubated with 10 μg/mL biotinylated anti-C1q mAbs for 45 min at 4 °C and washed again. Binding of anti-C1q mAbs to the cells was detected by incubating with 2 μg/mL streptavidin-AlexaFluor647 for 45 min at 4 °C. As positive control for C1q binding, polyclonal rabbit anti-C1q (DAKO) and BrilliantViolet421-labeled donkey anti-rabbit IgG (BioLegend) were used. After the final wash, the fluorescent signal on the cells was measured on a FACSCanto flow cytometer (BD Biosciences).

ELISA for Competition between anti-C1q mAbs and Purified SLE Antibodies. ELISA plates were coated with 10 μg/mL C1q in coating buffer overnight at 4 °C and subsequently blocked with PBS/1%BSA for 1 h at 37 °C. Competitor anti-C1q mAb at 64 μg/mL final concentration, or protein A-purified SLE antibodies at 5 mg/mL, was added to the plates in PTB and incubated 1 h at 37 °C. Without washing, biotinylated anti-C1q mAb was then added at concentration between 0.15 and 12 μg/mL depending on the concentration needed to obtain near saturation binding signal without competition. After incubation for 1 h at 37 °C, plates were washed and biotinylated anti-C1q mAb binding

was detected by 0.1 μg/mL streptavidin-HRP. Plates were developed by incubating with ABTS/0.015% H_2O_2, and absorbance was measured at 415 nm using a microplate reader. Percentage residual binding was calculated by dividing absorbance in presence of competition by absorbance in the absence of competition.

ELISA to Detect Binding of Anti-C1q mAbs to C1q Collagen-like Region and Globular Heads. ELISA plates were coated with C1q CLR made by limited proteolysis of purified serum C1q, recombinant single-chain GH domains (described in ref. 44) (both gifts from Nicole Thielens), or purified intact C1q at 10 μg/mL in coating buffer for 1 h at 37 °C. The plates were then blocked with PBS/1%BSA for 1 h at 37 °C, washed, and incubated with 4 μg/mL anti-C1q mAb, or 10 μg/mL for mAb 12F6, for 1 h at 37 °C. After washing, bound anti-C1q mAb was detected with 1:2000 rabbit anti-human IgG-HRP, plates were developed by incubating with ABTS/0.015% H_2O_2, and absorbance at 415 nm was measured using a microplate reader. Absorbance values for binding to intact C1q were set to 100% for each mAb to facilitate easier comparison.

Sample Preparation and Data Collection for Negative Stain Electron Tomography. C1q (270 μg/mL final concentration) was incubated with IgG1-anti-CD52-RGY (540 μg/mL final concentration) for 30 min at 4 °C. Monovalent, Fc-inactive anti-C1q bsAb combining 1F5 with control b12 (made as described for the solid-phase C1q inhibition ELISA; used at 90 μg/mL final concentration) was added and samples were incubated for another 30 min at 4 °C. Samples were purified using a Superdex 200 Increase 3.2/300 column (Cytiva). Column was equilibrated with PBS on an Äkta pure system (Cytiva). Size exclusion fractions were diluted 1:10 in water and loaded on freshly plasma-cleaned 200 mesh carbon-coated copper grids (Electron Microscopy Sciences) and incubated for 1 min, before blotting using Whatman paper. Samples were stained using 2% uranyl formate for 1 min. Negative stain tilt-series were collected on a FEI Tecnai T12 Biotwin with LaB6 source, operating at 120 kV on a FEI Eagle 4 k × 4 k CCD camera. Tilt series were collected using Xplore 3D (ThermoFisher Scientific) at 49,000× magnification and a pixel size of 4.546 Å using a continuous acquisition scheme from ±60° with a tilt increment of 3°. A total dose of 100 $e^-/Å^2$ and a defocus of −4 μm was used. Tracking and focusing were performed before every third image acquisition.

Tomogram Reconstruction. Alignment of cryo-electron tomography raw frames was performed using the "alignframes" command from the software program IMOD 4.11.13 (45). Additionally, IMOD was used to reconstruct negative stain tomograms using weighed back projected with a SIRT-like filter equivalent to five iterations. Tomograms were aligned using patch tracking. IgG1–C1q–1F5 maps were displayed on the tomographic slices using UCSF Chimera 1.16 (46).

ELISA for Complement Activation in the Presence of anti-C1q mAbs. IgG1 anti-DNP with RGY mutations for hexamer formation were coated on ELISA plates at 10 μg/mL in coating buffer for 1 h at 37 °C. The plates were blocked with PBS/1%BSA for 1 h at 37 °C, washed and incubated with 10 μg/mL C1q for 1 h at 37 °C. After washing, 50 μg/mL anti-C1q mAb was incubated in the wells for 1 h at 37 °C. The wells were washed, incubated with 1% NHS in RPMI 1640 (Gibco) for 1 h at 37 °C, and washed again. Deposited C5b-9 was detected using 333x diluted Mouse anti-C5b9 (clone aE11, DAKO) and Goat anti-Mouse-HRP (DAKO). Plates were developed with ABTS/0.015% H_2O_2 and absorbance at 415 nm was measured using a microplate reader.

ELISA for FcγRIIIa Binding in Presence of Anti-C1q mAbs. FcγRIIIa with a C-terminal 10xHis and BirA tags were produced in Freestyle 293-F cells (ThermoFisher), purified on a His-trap column (GE Life Sciences) and biotinylated with BirA as described previously (47). IgG1 anti-DNP with RGY mutations for hexamer formation were coated on ELISA plates at 10 μg/mL in coating buffer for 1 h at 37 °C. The plates were blocked with PBS/1%BSA for 1 h at 37 °C, washed and incubated with 10 μg/mL C1q for 1 h at 37 °C. After washing, 50 μg/mL anti-C1q mAb was incubated in the wells for 1 h at 37 °C. The wells were washed and then incubated with 3 μg/mL FcγRIIIa-biotin for 1 h at 37 °C. Detection of FcγRIIIa-biotin after washing was performed by incubating with 0.1 μg/mL streptavidin-HRP for 1 h at 37 °C. After adding ABTS/0.015% H_2O_2, absorbance at 415 nm was measured using a microplate reader.

Binding of Anti-C1q Opsonized Beads by THP-1 Cells. The THP-1 cell line (ATCC TIB-202) was cultured in RPMI (Gibco) with 10% FCS, 2 mM L-glutamine, 100 units/mL penicillin, and 100 μg/mL streptomycin (all Gibco). Cells were differentiated to a macrophage phenotype by incubating 100,000 cells/well in a 48-well plate with phorbol 12-myristate 13-acetate (PMA; Sigma-Aldrich) in the medium. After 3 d incubating at 37 °C, medium was replaced with PMA-free medium and cells were incubated for another 5 d. Yellow fluorescent 0.46-μm carboxyl beads (Spherotech) were loaded with IgM for 1 h at 37 °C, washed three times in PBS, and incubated with C1q for 1 h at 4 °C. After washing, beads suspension was incubated with anti-C1q mAb in serum-free medium for 1 h at 4 °C, after which the mixture was added to the differentiated THP-1 cells. Per well, 3 × 10^8 beads, incubated with 0.1 μg IgM, 0.5 μg C1q, and 0.2 μg anti-C1q mAb were added in a total volume of 200 μL serum-free medium. For experiments with Fc blocking reagent, cells were incubated with 10 μg/mL Human Fc block (BD Biosciences) for 10 min at room temperature before adding the beads suspension. Plates were centrifuged for 1 min at 100*g* to bring the beads in contact with the cells and were then incubated for 1 h at 37 °C to allow binding and phagocytosis of anti-C1q mAb-covered beads by the cells. The beads suspension was removed, and the cells were treated with trypsin (Gibco) to detach them from the plate. Cells were resuspended, washed in FACS buffer and then analyzed on a FACSCanto flow cytometer. Binding or phagocytosis was measured by FITC fluorescence. Differentiation of THP-1 cells was confirmed by increased expression of CD11b (by mouse anti-CD11b-APC, clone D12, BD Biosciences) and decreased expression of CD15 (by mouse anti-CD15-BV510, clone W6D3, BD Biosciences).

Phagocytosis of *S. aureus* by Human Neutrophils. Human polymorphonuclear (PMN) leukocytes were isolated freshly from blood of healthy donors by the Ficoll-Histopaque gradient method (48). In 96-well plates, mAmetrine-labeled *S. aureus* (49) (strain Newman Δ*spa/sbi;* 750,000 cells/well) was mixed with 1.5 μg/mL mAb [IgG4 with E430G mutation (24) against wall teichoic acid (WTA) and 6 μg/mL C1q in RPMI supplemented with 0.05% HSA. Plates were incubated for 15 min at 37 °C on an orbital shaker. Subsequently, anti-C1q mAbs were added at 10 μg/mL, and plates were incubated for another 15 min at 37 °C on an orbital shaker. Finally, PMN leukocyte cells were added at 75,000 cells/well to allow phagocytosis of opsonized bacteria. After 15-min incubation at 37 °C, phagocytosis was stopped by addition of 1% paraformaldehyde. Neutrophils were gated based on forward and sideward scatter, and the fluorescence of mAmetrine-labeled bacteria associated with neutrophils was acquired.

Statistical Analysis. Where applicable, statistical analysis of results was performed in GraphPad Prism software version 9.3. EC50 of anti-C1q mAb binding to C1q-coated ELISA was determined from an agonist vs. response curve with variable slope (four parameters). Significance for solid-phase C1q inhibition, complement activation, and FcγRIIIa binding was determined per anti-C1q mAb by one-way ANOVA followed by Dunnett's multiple comparisons test. A *P*-value below 0.05 was considered statistically significant.

Data, Materials, and Software Availability. All study data are included in the article and/or *SI Appendix*.

ACKNOWLEDGMENTS. We thank the patients, donors, doctors, and other technical staff in the Leiden University Medical Center (LUMC) for providing the samples. We are grateful to Nicole Thielens for supplying C1q CLR and GH domains. We thank Maartje Ruyken (University Medical Center Utrecht) for assistance in phagocytosis experiments. Furthermore, we thank the Flow Cytometry Core Facility of the LUMC for their help in cell sorting and flow cytometry experiments and Joost Bakker for aid in visualization. The project received funding from the European Research Council (ERC) under the European Union's Horizon 2020 research and innovation program (grant agreement No. 101001937, ERC-ACCENT) to S.H.M.R., and from the LUMC Research profile: Immunity, Infection and Tolerance to L.A.T.

Author affiliations: [a]Department of Immunology, Leiden University Medical Center, Leiden 2300 RC, The Netherlands; [b]Lava Therapeutics, Utrecht 3584 CM, The Netherlands; [c]Department of Cell and Chemical Biology, Leiden University Medical Center, Leiden 2300 RC, The Netherlands; [d]Department of Rheumatology, Leiden University Medical Center, Leiden 2300 RC, The Netherlands; [e]Department of Medical Microbiology, University Medical Center, Utrecht 3584 CX, The Netherlands; [f]Sanquin Diagnostic Services, Amsterdam 1066 CX, The Netherlands; [g]Department of Experimental Immunohematology, Sanquin Research, Amsterdam 1066 CX, The Netherlands; and [h]Gyes BV, Naarden 1411 DC, The Netherlands

Author contributions: D.J.D., F.S.v.d.B., T.H.S., P.W.H.I.P., and L.A.T. designed research; D.J.D., L.A., R.Z., J.P., and L.d.V. performed research; C.S.M.K., L.M.S., J.W.D., K.A.G., A.Z., and G.V. contributed new reagents/analytic tools; D.J.D., F.S.v.d.B., L.A., L.d.V., T.H.S., and L.A.T. analyzed data; and D.J.D., F.S.v.d.B., L.A., C.S.M.K., L.M.S., S.H.M.R., G.V., T.H.S., P.W.H.I.P., and L.A.T. wrote the paper.

1. D. Ricklin, G. Hajishengallis, K. Yang, J. D. Lambris, Complement: A key system for immune surveillance and homeostasis. *Nat. Immunol.* **11**, 785 (2010).
2. R. A. van Schaarenburg *et al.*, Marked variability in clinical presentation and outcome of patients with C1q immunodeficiency. *J. Autoimmun.* **62**, 39–44 (2015).
3. D. J. Dijkstra, J. V. Joeloemsingh, I. M. Bajema, L. A. Trouw, Complement activation and regulation in rheumatic disease. *Semin. Immunol.* **45**, 101339 (2019).
4. M. A. Dragon-Durey, C. Blanc, M. C. Marinozzi, R. A. van Schaarenburg, L. A. Trouw, Autoantibodies against complement components and functional consequences. *Mol. Immunol.* **56**, 213–221 (2013).
5. F. S. van de Bovenkamp, D. J. Dijkstra, C. van Kooten, K. A. Gelderman, L. A. Trouw, Circulating C1q levels in health and disease, more than just a biomarker. *Mol. Immunol.* **140**, 206–216 (2021).
6. M. A. Seelen, L. A. Trouw, M. R. Daha, Diagnostic and prognostic significance of anti-C1q antibodies in systemic lupus erythematosus. *Curr. Opin. Nephrol. Hypertens.* **12**, 619–624 (2003).
7. L. A. Trouw *et al.*, Anti-C1q autoantibodies deposit in glomeruli but are only pathogenic in combination with glomerular C1q-containing immune complexes. *J. Clin. Invest.* **114**, 679–688 (2004).
8. I. E. Coremans *et al.*, Changes in antibodies to C1q predict renal relapses in systemic lupus erythematosus. *Am. J. Kidney Dis.* **26**, 595–601 (1995).
9. M. Trendelenburg, J. Marfurt, I. Gerber, A. Tyndall, J. A. Schifferli, Lack of occurrence of severe lupus nephritis among anti-C1q autoantibody-negative patients. *Arthritis Rheum.* **42**, 187–188 (1999).
10. D. Saadoun *et al.*, Anti-C1q antibodies in hepatitis C virus infection. *Clin. Exp. Immunol.* **145**, 308–312 (2006).
11. C. Magro-Checa *et al.*, Complement levels and anti-C1q autoantibodies in patients with neuropsychiatric systemic lupus erythematosus. *Lupus* **25**, 878–888 (2016).
12. F. J. Beurskens, R. A. van Schaarenburg, L. A. Trouw, C1q, antibodies and anti-C1q autoantibodies. *Mol. Immunol.* **68**, 6–13 (2015).
13. J. Kohro-Kawata, M. H. Wener, M. Mannik, The effect of high salt concentration on detection of serum immune complexes and autoantibodies to C1q in patients with systemic lupus erythematosus. *J. Rheumatol.* **29**, 84–89 (2002).
14. S. Uwatoko *et al.*, C1q solid-phase radioimmunoassay: Evidence for detection of antibody directed against the collagen-like region of C1q in sera from patients with systemic lupus erythematosus. *Clin. Exp. Immunol.* **69**, 98–106 (1987).
15. M. D. Golan, R. Burger, M. Loos, Conformational changes in C1q after binding to immune complexes: Detection of neoantigens with monoclonal antibodies. *J. Immunol.* **129**, 445–447 (1982).
16. S. Uwatoko *et al.*, Characterization of C1q-binding IgG complexes in systemic lupus erythematosus. *Clin. Immunol. Immunopathol.* **30**, 104–116 (1984).
17. J. S. Kleer *et al.*, Epitope-specific anti-C1q autoantibodies in systemic lupus erythematosus. *Front. Immunol.* **12**, 761395 (2021).
18. I. Tsacheva, M. Radanova, N. Todorova, T. Argirova, U. Kishore, Detection of autoantibodies against the globular domain of human C1q in the sera of systemic lupus erythematosus patients. *Mol. Immunol.* **44**, 2147–2151 (2007).
19. M. Radanova *et al.*, Anti-C1q autoantibodies specific against the globular domain of the C1qB-chain from patient with lupus nephritis inhibit C1q binding to IgG and CRP. *Immunobiology* **217**, 684–691 (2012).
20. D. Vanhecke *et al.*, Identification of a major linear C1q epitope allows detection of systemic lupus erythematosus anti-C1q antibodies by a specific peptide-based enzyme-linked immunosorbent assay. *Arthritis Rheum.* **64**, 3706–3714 (2012).
21. V. Giudicelli, X. Brochet, M. P. Lefranc, IMGT/V-QUEST: IMGT standardized analysis of the immunoglobulin (IG) and T cell receptor (TR) nucleotide sequences. *Cold Spring Harb. Protoc.* **2011**, 695–715 (2011).
22. C. A. Ogden *et al.*, C1q and mannose binding lectin engagement of cell surface calreticulin and CD91 initiates macropinocytosis and uptake of apoptotic cells. *J. Exp. Med.* **194**, 781–795 (2001).
23. R. Fong *et al.*, Structural investigation of human *S. aureus*-targeting antibodies that bind wall teichoic acid. *MAbs* **10**, 979–991 (2018).
24. S. A. Zwarthoff *et al.*, C1q binding to surface-bound IgG is stabilized by C1r(2)s(2) proteases. *Proc. Natl. Acad. Sci. U.S.A.* **118**, e2102787118 (2021).
25. Q. Y. Fang *et al.*, Anti-C1q antibodies and IgG subclass distribution in sera from Chinese patients with lupus nephritis. *Nephrol. Dial. Transplant* **24**, 172–178 (2009).
26. I. E. Coremans, M. R. Daha, E. A. van der Voort, C. E. Siegert, F. C. Breedveld, Subclass distribution of IgA and IgG antibodies against Clq in patients with rheumatic diseases. *Scand. J. Immunol.* **41**, 391–397 (1995).
27. M. H. Van Regenmortel *et al.*, Measurement of antigen–antibody interactions with biosensors. *J. Mol. Recognit.* **11**, 163–167 (1998).
28. J. J. Wisnieski, S. M. Jones, Comparison of autoantibodies to the collagen-like region of C1q in hypocomplementemic urticarial vasculitis syndrome and systemic lupus erythematosus. *J. Immunol.* **148**, 1396–1403 (1992).
29. T. H. Sharp *et al.*, Insights into IgM-mediated complement activation based on in situ structures of IgM–C1–C4b. *Proc. Natl. Acad. Sci. U.S.A.* **116**, 11900–11905 (2019).
30. D. Ugurlar *et al.*, Structures of C1–IgG1 provide insights into how danger pattern recognition activates complement. *Science* **359**, 794–797 (2018).
31. P. F. Kerkman *et al.*, Identification and characterisation of citrullinated antigen-specific B cells in peripheral blood of patients with rheumatoid arthritis. *Ann. Rheum. Dis.* **75**, 1170–1176 (2016).
32. M. L. Gonzalez, M. B. Frank, P. A. Ramsland, J. S. Hanas, F. J. Waxman, Structural analysis of IgG2A monoclonal antibodies in relation to complement deposition and renal immune complex deposition. *Mol. Immunol.* **40**, 307–317 (2003).
33. G. Wang *et al.*, Molecular basis of assembly and activation of complement component C1 in complex with immunoglobulin G1 and antigen. *Mol. Cell* **63**, 135–145 (2016).
34. C. S. M. Kramer *et al.*, Generation and reactivity analysis of human recombinant monoclonal antibodies directed against epitopes on HLA-DR. *Am. J. Transplant* **20**, 3341–3353 (2020).
35. R. H. Zubler *et al.*, Mutant EL-4 thymoma cells polyclonally activate murine and human B cells via direct cell interaction. *J. Immunol.* **134**, 3662–3668 (1985).
36. L. C. Lighaam *et al.*, Phenotypic differences between IgG4+ and IgG1+ B cells point to distinct regulation of the IgG4 response. *J. Allergy Clin. Immunol.* **133**, 267–270.e1-6 (2014).
37. S. Heidt *et al.*, Calcineurin inhibitors affect B cell antibody responses indirectly by interfering with T cell help. *Clin. Exp. Immunol.* **159**, 199–207 (2010).
38. C. S. M. Kramer *et al.*, Recombinant human monoclonal HLA antibodies of different IgG subclasses recognising the same epitope: Excellent tools to study differential effects of donor-specific antibodies. *Hla* **94**, 415–424 (2019).
39. X. Brochet, M. P. Lefranc, V. Giudicelli, IMGT/V-QUEST: The highly customized and integrated system for IG and TR standardized V-J and V-D-J sequence analysis. *Nucleic Acids Res.* **36**, W503–508 (2008).
40. M. Lo *et al.*, Effector-attenuating substitutions that maintain antibody stability and reduce toxicity in mice. *J. Biol. Chem.* **292**, 3900–3908 (2017).
41. A. F. Labrijn *et al.*, Controlled Fab-arm exchange for the generation of stable bispecific IgG1. *Nat. Protoc.* **9**, 2450–2463 (2014).
42. C. A. Diebolder *et al.*, Complement is activated by IgG hexamers assembled at the cell surface. *Science* **343**, 1260–1263 (2014).
43. L. A. Trouw, S. C. Nilsson, I. Gonçalves, G. Landberg, A. M. Blom, C4b-binding protein binds to necrotic cells and DNA, limiting DNA release and inhibiting complement activation. *J. Exp. Med.* **201**, 1937–1948 (2005).
44. C. Moreau *et al.*, Structural and functional characterization of a single-chain form of the recognition domain of complement protein C1q. *Front. Immunol.* **7**, 79 (2016).
45. J. R. Kremer, D. N. Mastronarde, J. R. McIntosh, Computer visualization of three-dimensional image data using IMOD. *J. Struct. Biol.* **116**, 71–76 (1996).
46. E. F. Pettersen *et al.*, UCSF Chimera–A visualization system for exploratory research and analysis. *J. Comput. Chem.* **25**, 1605–1612 (2004).
47. T. Šuštić *et al.*, Immunoassay for quantification of antigen-specific IgG fucosylation. *EBioMedicine* **81**, 104109 (2022).
48. E. Boero *et al.*, Use of flow cytometry to evaluate phagocytosis of *Staphylococcus aureus* by human neutrophils. *Front. Immunol.* **12**, 635825 (2021).
49. A. R. Cruz *et al.*, Staphylococcal protein A inhibits complement activation by interfering with IgG hexamer formation. *Proc. Natl. Acad. Sci. U.S.A.* **118**, e2016772118 (2021).